Effect of Turbulence Intensity on the Performance Characteristics of Large-Scale Wells Turbine

P. Madhan Kumar[1], Abdus Samad[1*]

Wave Energy and Fluids Engineering Laboratory, Department of Ocean Engineering, Indian Institute of Technology Madras, Chennai 600036, India

[1]madyypts@gmail.com

[1*]samad@iitm.ac.in

Abstract— **Wells turbine is a self-rectifying axial air turbine, which consists of symmetrical aerofoil at 90° stagger. It is used to extract power from the bidirectional airflow inside an oscillating water column. Generally, the performance of the turbomachines is affected by the turbulence intensity. In this numerical study, the effect of turbulence intensity on the performance of large-scale Wells turbine is investigated. Different values of turbulent intensities were applied at the inlet and their influence on the aerodynamic characteristics is analysed. A single blade with periodic boundary condition is taken as the computational domain for numerical analyses. The simulation results of the reference geometry were compared with existing experiment and numerical results. The performances of the Wells turbine with different turbulent intensities were computed by solving Reynolds-averaged Navier-Stokes (RANS) equations. Finally, the results were compared and analysed. It is found that the large-scale Wells turbine (LSWT) performance is unaffected by the varying inlet turbulence intensity. Furthermore, a marginal improvement in the performance was observed with an increase in turbulence intensity.**

Keywords— **Wave energy, OWC, Wells turbine, CFD, Turbulence intensity**

I. INTRODUCTION

With the depletion of global fossil fuel resources at an alarming rate, the necessity for commercial exploitation of renewable energy sources is inevitable. The ocean holds a vast amount of untapped clean source of renewable energy in the form of tides, currents, waves, and temperature gradients. Most of the commercially deployed ocean energy projects are based on tidal energy power plants, while the commercial implementation of wave energy is still in the preliminary stage [1]. The feasibility of wave energy commercialization can be improved by enhancing the performance of the wave energy converters (WEC) [2]. There are various methods are available to extract the wave energy, one of them is oscillating water column (OWC). The OWC consists of partially immersed structure open to the water underneath, where the incoming waves interact with the trapped air inside to drive the air turbine [3]. The Wells turbine is used as the power take-off device in the OWC. It extracts the energy from the oscillating bi-directional airflow inside the OWC and provides unidirectional torque irrespective of the direction of airflow. The Wells turbine uses symmetrical airfoil profiles at 90º stagger angle. It is a self-rectifying air turbine; hence, there is no need of guide vanes to make the turbine rotation unidirectional. On the contrary, the Wells turbine has some integral disadvantages such as noisy operation, poor starting characteristics, and narrow operating range. The operation of Wells turbine depends on various parameters such as solidity, tip clearance, Reynolds number, hub to tip ratio, aspect ratio, and inlet turbulent intensity etc. The turbulence intensity influences the performance of the turbomachines significantly. There is only a handful of literature available on the influence of turbulence intensity on the operating characteristics of Wells turbine. Raghunathan et al. [4] studied the effects of turbulence intensity on the aerodynamic performance of Wells turbine and concluded that it is unaffected by small changes in turbulence intensity. The reason behind this is the absolute velocity at the inlet based on which the inlet turbulence intensity is defined is relatively smaller compared to the rotor velocity [5]. The biplane Wells turbine is affected by the changes of turbulence intensity compared to the monoplane Wells turbine [6]. These studies are performed on a small-scale Wells turbine with a tip diameter of 200 mm and a chord length of 65 mm. The influence of turbulence intensity on the aerodynamic characteristics of the LSWT has not been analysed so far. In this study, the present numerical results of the reference turbine are compared with both experimental and numerical results to ensure the accuracy of numerical simulations performed. The value of turbulence intensity at the inlet is varied and their effect on the aerodynamic characteristics of the Wells turbine is analysed. The flow field analysis is also explained in detail with the help of post-processed figures to understand the fluid dynamics.

II. WELLS TURBINE

The schematic of Wells turbine is shown in Fig.1. The geometry used in the work of Torresi et al. [7] is selected as the reference geometry. The specifications of the reference turbine geometry are presented in Table 1. The reference geometry consists of NACA0015 as the blade profile. It is a symmetrical airfoil with a maximum thickness of 15% chord length and zero camber. The unidirectional rotation of Wells turbine is due to the symmetrical nature of the blade profiles

used. The chord of the blades is oriented along the axis of rotation which is different from the conventional turbines.

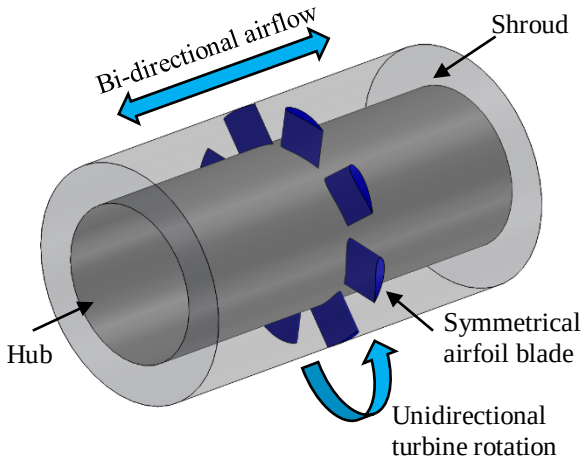

Fig. 1 Wells Turbine

Table 1. Reference Turbine Specifications

Blade profile	NACA0015
Maximum thickness	15% chord length
Maximum thickness location	30% chord length
Number of blades	8
Chord length (C)	125 mm
Tip diameter	300 mm
Hub diameter	200 mm
Solidity	0.64
Tip clearance	1.25 mm
Rotation speed	2000 rpm

A. Performance parameters of a Wells Turbine

The following non-dimensional parameters are used to analyse the Wells turbine performance [7].

Torque coefficient:

$$T^* = \frac{T}{\rho\omega^2 R_{tip}^5} \quad (1)$$

Stagnation pressure drop coefficient:

$$\Delta p^* = \frac{\Delta p_o}{\rho\omega^2 R_{tip}^2} \quad (2)$$

Efficiency:

$$\eta = \frac{T\omega}{Q\Delta p_o} \quad (3)$$

Flow coefficient:

$$U^* = \frac{U_\infty}{U_{tip}} \quad (4)$$

Where T is the shaft torque, ρ is the density of air (1.225 kg/m^3), ω is the angular velocity of the rotor (209.4 rad/s), R_{tip} is the blade tip radius (300 mm), Δp_o is the stagnation pressure drop across the turbine, Q is the volumetric discharge, U_∞ is the free stream velocity and U_{tip} is the blade tip velocity. The non-dimensional parameters T^*, Δp^* and η are plotted against U^* to obtain the performance characteristics of Wells turbine.

B. Turbulence Intensity

It is described as the ratio of root mean square of fluctuating velocity components (u') and average of the mean velocity components(U) [8]. It can be expressed as

$$I = \frac{u'}{U} \quad (5)$$

Where

$$u' = \sqrt{\frac{1}{3}(u_x'^2 + u_y'^2 + u_z'^2)} \quad (6)$$

$$U = \sqrt{(\bar{u}_x^2 + \bar{u}_y^2 + \bar{u}_z^2)} \quad (7)$$

It is also known as level or degree of turbulence [9]. To assess the influence of inlet turbulence intensity, three values of turbulence intensity is defined and the numerical simulations were performed for the entire flow range. The values of inlet turbulence intensity selected for this study are 5% (low), 15% (medium) and 30% (high).

III. Numerical Methodology

A single blade with the periodic interface is chosen as the flow domain for numerical analyses (Fig. 2). A right-handed Cartesian system is adopted, where the positive x, y, z-axis represents the chordwise, downstream and spanwise directions respectively. The upstream and downstream length of the computation domain is taken as 4C and 6C respectively. The discretization of the computational domain is done with the unstructured tetrahedral elements using ICEM CFD software. The unstructured mesh is suitable for meshing complex geometries and it is less time-consuming. To resolve the viscous sublayer, 20 layers of prism elements are generated around the blade with an expansion ratio of 1.2. The Y+ value is maintained less than 1 and the first cell height is taken as 0.011 mm. The discretized computational domain and the prism layers around the blade are presented in Fig. 3. The numerical analyses are performed by solving three dimensional steady incompressible RANS equations using ANSYS CFX 14.5. The boundary conditions are implemented in ANSYS CFX Pre. The imposed boundary conditions are presented in Table 2. The ANSYS CFX 14.5 is a coupled solver and it solves the aerodynamic equations of (u,v,w,p) as a single system [10]. It ensures robustness and better convergence with a minimum number of iterations.

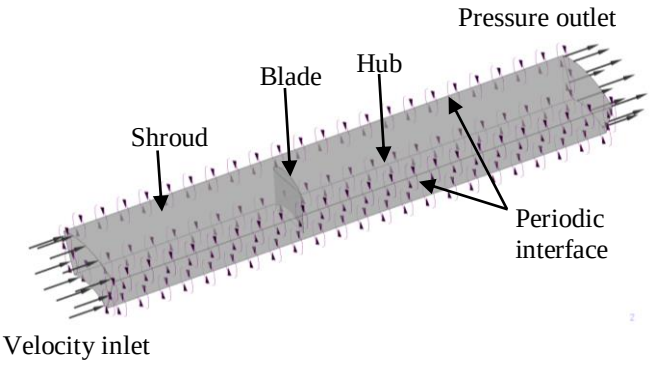

Fig. 2 Computational Domain

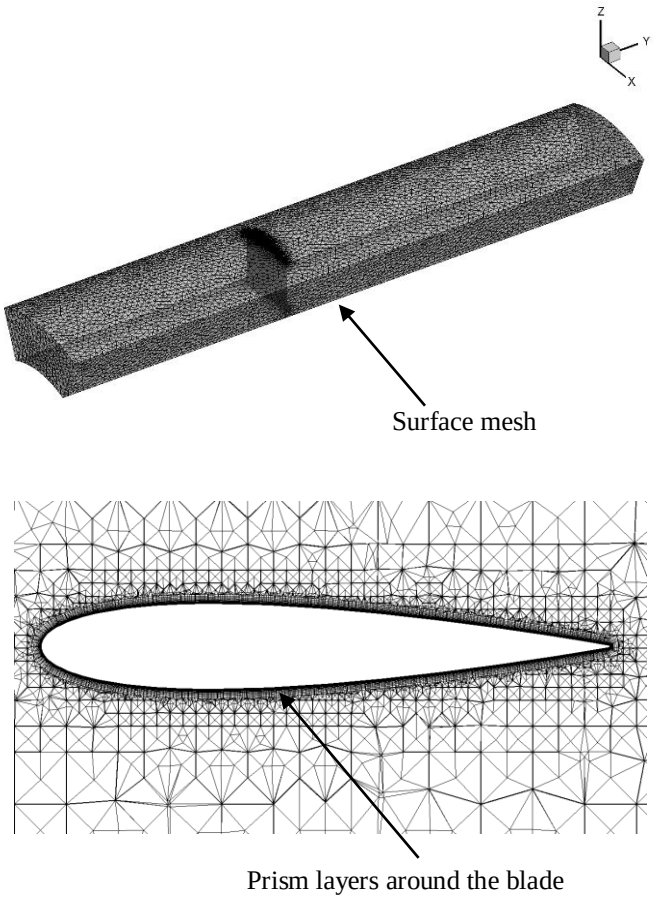

Fig. 3 Discretized Computational Domain

The k-ω SST with automatic wall function is selected as turbulence model as it suitable for flows with adverse pressure gradient and separation. It combines the advantages of k-ε and k-ω turbulence models and activates k-ω model closer to the wall and k-ε model away from the wall [11]. Turbulence intensity at the inlet is fixed as 5%. High-resolution advection scheme with second-order accuracy is used for spatial discretization. The numerical simulations are run up to 2000 iterations. The numerical simulations are performed in Virgo supercluster available at Indian Institute of Technology Madras.

Table 2. Boundary Conditions

Parameter	Description
Working fluid	Air
Nature of flow	Incompressible
Reference pressure	1 atm
Inlet	Velocity inlet
Outlet	Pressure outlet
Blade and hub	No-slip wall
Shroud	Contra-rotating no-slip wall
Turbulence model	k-ω SST
Residual criteria	1e-5

IV. Results and Discussion

A. Grid Independence Study

The grid independency study is necessary to select the grid with optimum mesh size since the increase in a number of elements increases the computational time taken for simulations. To perform the test, grids are refined from 1.46 million elements to 7.14 million elements. The number of elements is increased such that each grid is 1.5 times finer than the previous grid. Fig 4 shows the grid independency study conducted at U^*=0.125 at which the peak efficiency occurs in case of the reference case. The maximum deviation of efficiency is 5.5% and it is within the acceptable range, hence the grid with 3.07 million elements is chosen as the optimum grid and it is used for the numerical analyses performed in this study.

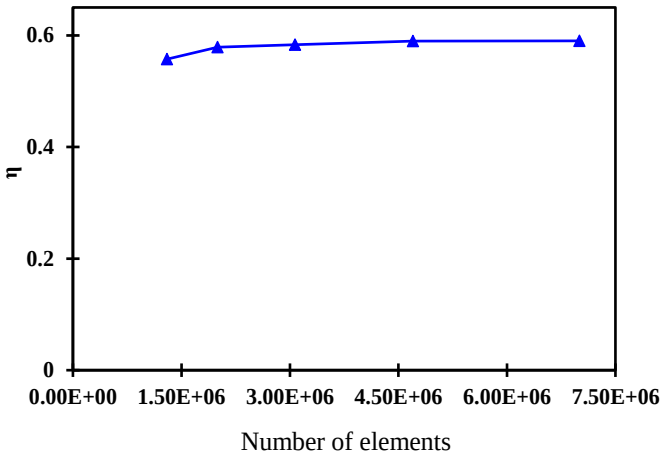

Fig. 4 Grid Dependency Test at Flow Coefficient Corresponding to Maximum Efficiency (U^*=0.125)

B. CFD Validation

To validate the accuracy of the CFD analyses performed, the present results are compared with the existing experiment [12] and CFD results [13,7,14,15]. The CFD validation of present numerical study is shown in Fig 5. The present result follows the same trend as the existing

experiment and CFD results, however, the discrepancy is observed with the results of Shaaban et al. [14] since the stall phenomenon is not captured and the value of torque and efficiency increases after flow coefficient U^*=0.225.

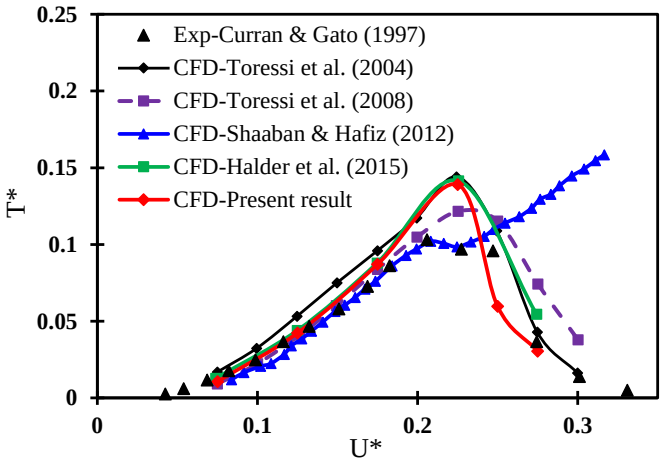

a) Torque Coefficient

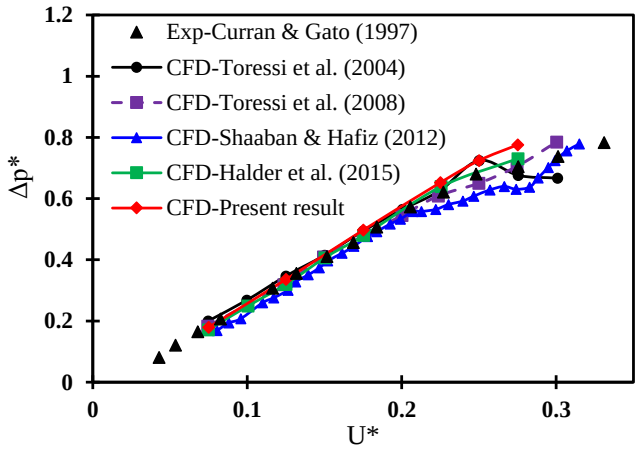

b) Stagnation Pressure Drop Coefficient

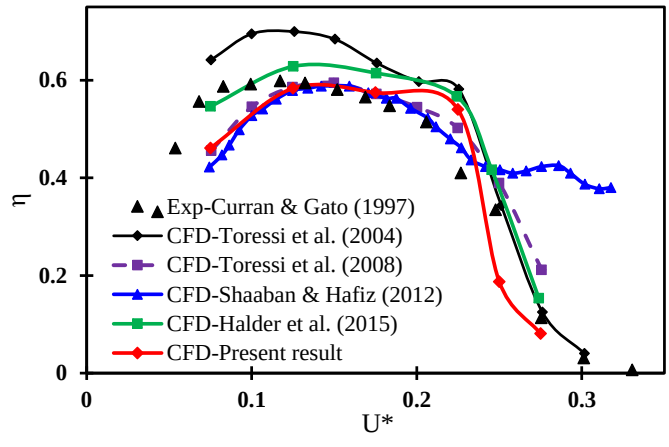

c) Efficiency

Fig. 5 CFD Validation

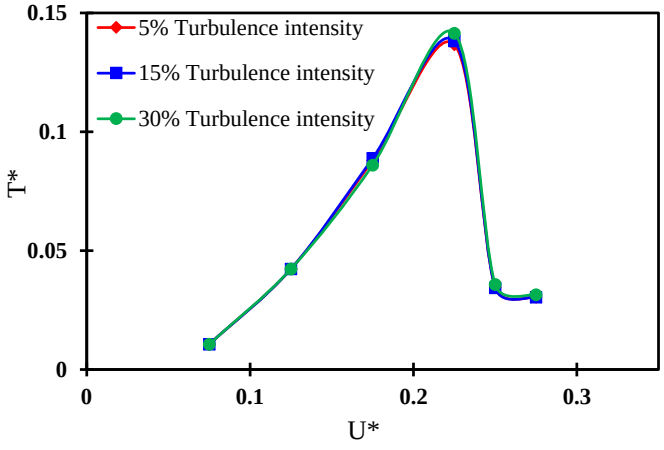

a) Torque Coefficient

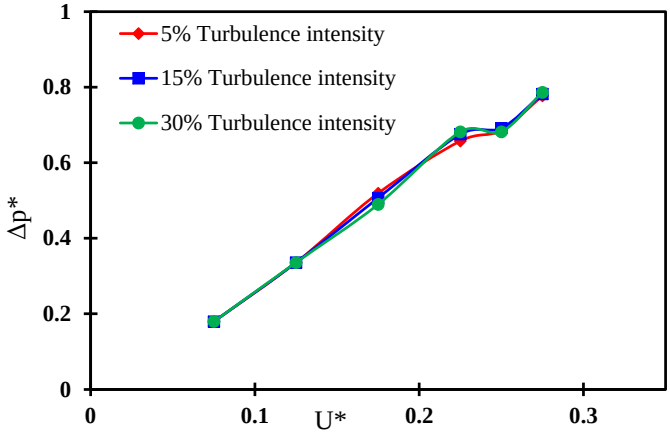

b) Stagnation Pressure Drop Coefficient

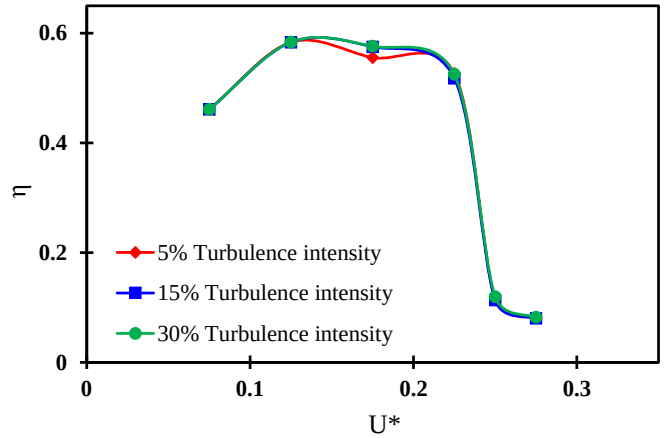

c) Efficiency

Fig. 6 Performance of Wells Turbine with Different Values of Turbulent Intensity at Inlet

C. Effect of Turbulence Intensity

To study the effect of turbulence intensity on the performance of Wells turbine, the three values of inlet turbulence intensity such as 5%, 15%, and 30% is selected and the numerical simulations are performed. To impose different values of turbulence intensities at the inlet, the intensity and auto compute length option is selected in ANSYS CFX-Pre boundary details and all other parameters are kept same for the numerical analyses. The performance characteristics of Wells turbine with varying turbulence intensity is presented in Fig 6. There is no significant difference is observed in the torque coefficient and the stagnation pressure drop coefficient with an increase in turbulence intensity (Fig 6a and 6b). Moreover, the peak torque coefficient is increased slightly with an increase in turbulence intensity. Similarly, the peak efficiency is improved marginally at an increased level of turbulence intensity (30%). These results are in agreement with the study of Raghunathan [5], where he reported that the monoplane Wells turbine is less sensitive to the inlet turbulence intensity.

Moreover, in this study, LSWT is subjected to varying turbulence intensities at the inlet is found to be less sensitive to inlet turbulence similar to the scaled Wells turbine, and no significant deviation is witnessed. The surface streamlines on the blade suction side (SS) is given in Fig 7. At low flow coefficient (FC) U^*=0.075, the flow is completely attached to the blade for all levels of inlet turbulence intensity and it can be seen from the figure that the streamlines are uniform throughout the SS of the blade. At FC 0.225, flow separation occurs near the trailing edge (TE) of the blade for all cases. However, at this FC, the peak torque is obtained due to a higher incidence of the incoming flow. It is evident that the separated region decreases with the increase in inlet turbulence intensity and it explains the marginal improvement in torque at a high level of turbulence intensities in Fig 6. The incidence increases with increase in flow coefficient and at higher incidence, the separation point is shifted towards the leading edge (LE) from the trailing edge (TE) and flow separation takes place.

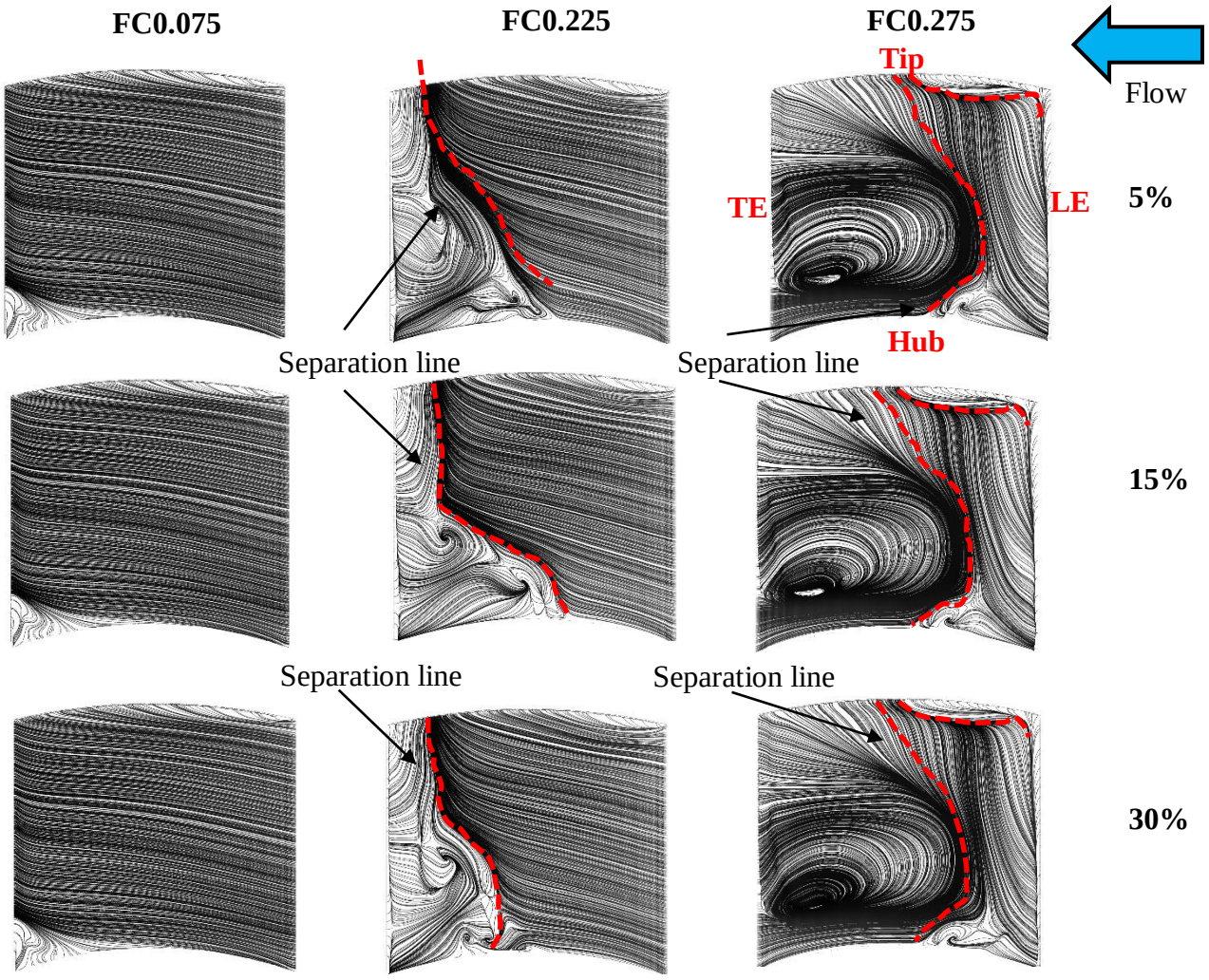

Fig. 7 Surface Streamlines on the Blade Suction Surface

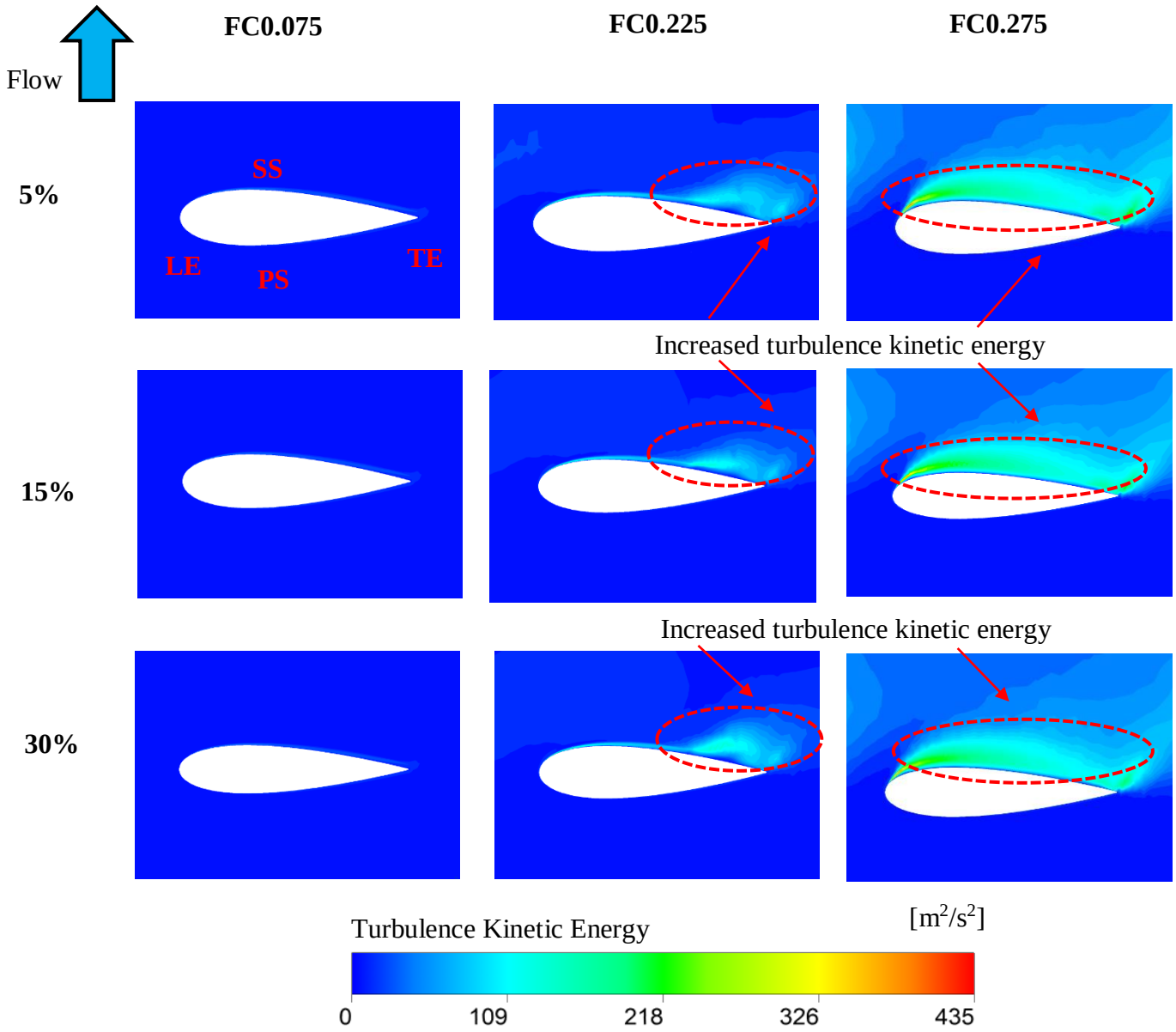

Fig. 8 Turbulence Kinetic Energy Contour at the Blade Midspan

At high FC (U^*=0.275), the separation line is moved towards the LE and the flow is completely separated for all the cases. The tip vortex is significantly increased at high FC due to a higher incidence. This flow separation implicates stall which is denoted by a rapid drop in torque and efficiency (Fig 6a & 6c). Fig 8 shows the turbulence kinetic energy contour at the blade midspan for different levels of inlet turbulence intensity. At low FC, the turbulence kinetic energy (TKE) is less significant for all levels of turbulence intensity. The increase in TKE indicates flow separation and at FC 0.225 increased TKE can be observed at SS of TE for all cases. This is in agreement with the trailing edge flow separation shown in Fig 7. With further increase in FC, the increased TKE advances in the direction of LE from TE and engulfs the SS of the blade for all the three cases. It implicates complete flow separation and stall, which can be verified from Fig 6 and 7. To corroborate the claims made, streamlines at the blade midspan is also analysed (Fig 9). As discussed earlier, at low FC the flow is fully attached for all the cases. At FC 0.225, flow separation is noticeable at the TE for all the cases. At FC 0.275, the separated region is visible on the SS of the blade surface for the three cases. This substantiates the results obtained before. There is no significant difference is observed for the performance of Wells turbine with different levels of inlet turbulence intensities. This is due to the absolute velocity used for calculating turbulence intensity is a fraction of the rotor relative velocity [6]. Moreover, it is evident that the LSWT is also less sensitive to the inlet turbulence intensity similar to the scaled Wells turbine used by Raghunathan [5].

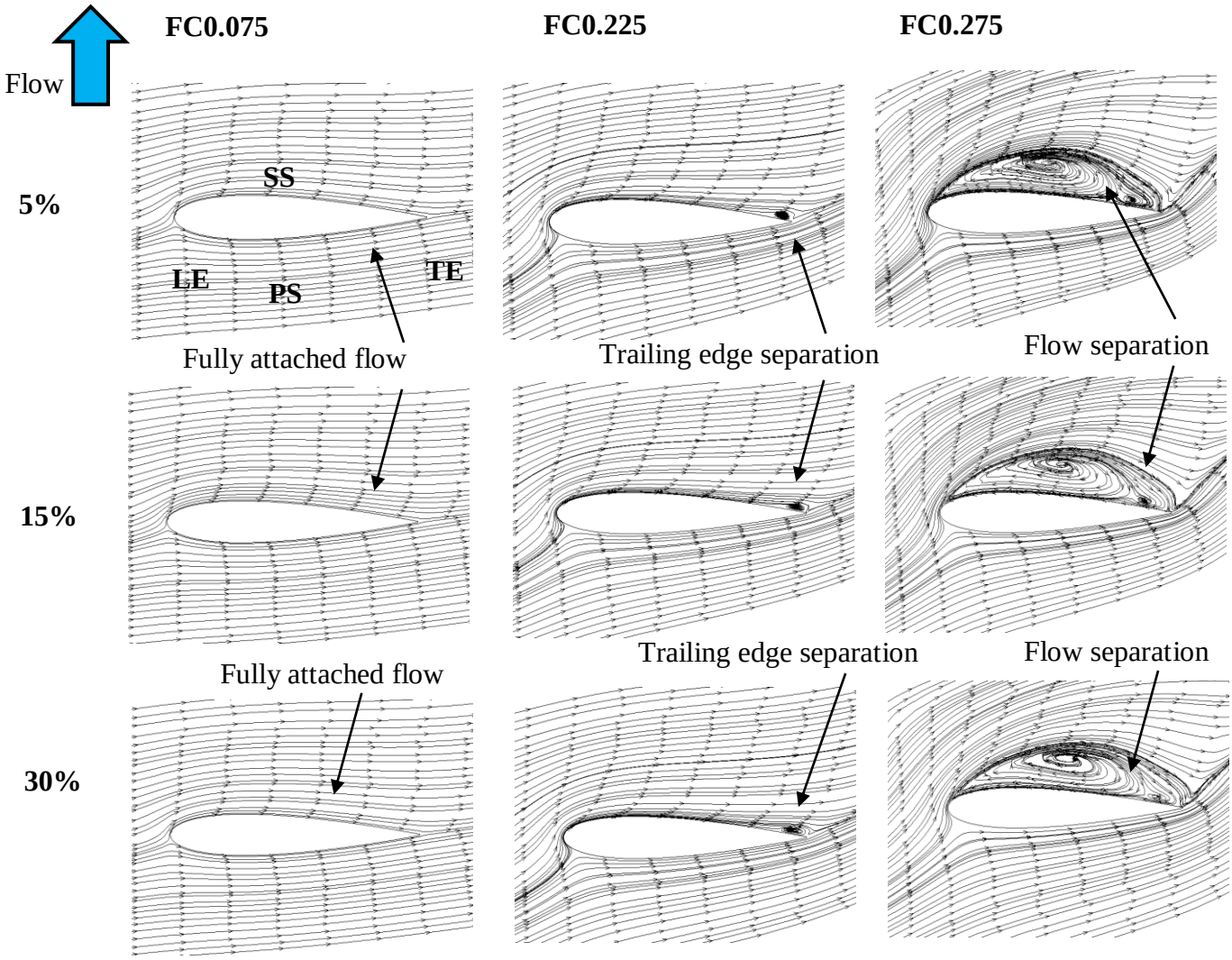

Fig. 9 Velocity Streamlines at the Blade Midspan

In addition, a marginal improvement in the performance of Wells turbine is observed at high values of turbulence intensity at the inlet.

V. Conclusion

In this study, the effect of turbulence intensity on the large-scale Wells turbine performance was presented. Various values of turbulence intensity was studied and the flow field was investigated using post-processed results. The prominent findings in this study are summarized as follows.

- The present numerical results matched significantly with the experiment and CFD results.
- The performance of Wells turbine is computed for different inlet turbulence intensity values such as 5%, 15%, and 30%.
- There is no significant difference is observed in the performance of Wells turbine for varying turbulence intensity values. The performance of the large-scale Wells turbine remained unaffected by the varying inlet turbulence intensity similar to the scaled Wells turbine.
- A marginal improvement in performance is observed with increase in turbulence intensity.

VI. References

1. Secretariat, R., 2017. "Renewables 2017 Global Status Report". REN21, Paris, Tech. Rep
2. Astariz, S., and G. Iglesias. "The economics of wave energy: A review." *Renewable and Sustainable Energy Reviews*, vol. 45, pp. 397–408, 2015.
3. Falnes, Johannes. *Ocean waves and oscillating systems: linear interactions including wave-energy extraction*. Cambridge university press, 2002.
4. Raghunathan, S., T. Setoguchi, and K. Kaneko. "The Wells air turbine subjected to inlet flow distortion and high levels of turbulence."

International journal of heat and fluid flow, vol. 8, no. 2, pp. 165-167, 1987

5. Raghunathan, S., "The Wells air turbine for wave energy conversion". *Progress in Aerospace Sciences*, vol. 31, no. 4, pp. 335-386, 1995.
6. Raghunathan, S., T. Setoguchi, and K. Kaneko. "The effect of inlet conditions on the performance of Wells turbine." *Journal of Energy Resources Technology*, vol. 111, no. 1, pp. 37-42, 1989.
7. Torresi, M., Camporeale, S. M., Strippoli, P. D., & Pascazio, G., "Accurate numerical simulation of a high solidity Wells turbine". *Renewable Energy*, vol. 33, no. 4, pp. 735-747, 2008.
8. Fluent, Ansys. "*12.0 Theory Guide*". Ansys Inc. 2009.
9. Schlichting, Hermann, Klaus Gersten, Egon Krause, and Herbert Oertel. *Boundary-layer theory*. New York: McGraw-Hill, 1955, vol. 7.
10. CFX, ANSYS, "*Solver Theory Guide.* Ansys. Inc., Canonsburg, PA., 2011.
11. Menter, F. R., "Two-equation eddy-viscosity turbulence models for engineering applications". *AIAA journal*, vol. 32, no. 8, pp. 1598-1605, 1994.
12. Curran, R., & Gato, L. M. C., "The energy conversion performance of several types of Wells turbine designs". *Proceedings of the Institution of Mechanical Engineers, Part A: Journal of Power and Energy*, vol. 211, no. 2, pp. 133-145, 1997.
13. Torresi, M., Camporeale, S. M., Pascazio, G., & Fortunato, B., "Fluid dynamic analysis of a low solidity Wells turbine". *In 59 Congresso ATI*, Genova, Italy, 2004.
14. Shaaban, S., & Hafiz, A. A., "Effect of duct geometry on Wells turbine performance". *Energy Conversion and Management*, vol. 61, pp. 51-58, 2012
15. Halder, P., Samad, A., Kim, J. H., & Choi, Y. S., "High performance ocean energy harvesting turbine design–A new casing treatment scheme". *Energy*, vol. 86, pp. 219-231, 2015.